Scientia Iranica B (2013) 20(6), 1781–1791

Sharif University of Technology
**Scientia Iranica**
*Transactions B: Mechanical Engineering*
www.scientiairanica.com

*Research Note*

# Lycopodium dust flame characteristics considering char yield

**M. Bidabadi**[a], **S.A. Mostafavi**[a,1,*], **H. Beidaghy Dizaji**[b] **and F. Faraji Dizaji**[a]

a. *School of Mechanical Engineering, Department of Energy Conversion, Combustion Research Laboratory, Iran University of Science and Technology, Tehran 16887, Iran.*
b. *School of Mechanical Engineering, Department of Aerospace Engineering, Iran University of Science and Technology, Tehran 16887, Iran.*

Received 25 December 2011; received in revised form 10 April 2013; accepted 15 July 2013

**KEYWORDS**
Analytical model;
Lycopodium particle;
Flame temperature;
Burning velocity;
Char content.

**Abstract.** Organic dust flames deal with a field of science in which many complicated phenomena like pyrolysis or devolatization of solid particles and the combustion of volatile and char particles take place. One-dimensional flame propagation in the cloud of a fuel mixture has been analyzed, in which the flame structure is divided into three zones: Preheat zone, reaction zone and post flame zone. It is assumed that particles pyrolyze first to yield a fuel mixture consisting of gaseous and charry fuel. In this research, the effect of char content on the pyrolysis process has been taken into account and a novel non-linear burning velocity correlation is obtained. Our results are in reasonable agreement with experimental data.

## 1. Introduction

Nowadays, the greenhouse effect is one of the most challenging issues for the human environment, and $CO_2$ is an important greenhouse gas. By increasing electricity consumption, $CO_2$ generation rate increases, and scientists are eager to find new approaches to generate electricity with no $CO_2$ production. Also, human activity produces much waste, like agricultural and municipal solid waste, an excessive amount of which threatens the health of humans and other life forms. The Stirling engine is one of the best solutions for both of these problems. These engines help to get rid of agricultural waste and also produce heat and power without increasing the amount of $CO_2$ in the atmosphere. The Stirling engines are fed by a micro-scale biomass up to 500 micrometers to enhance their efficiency. Furthermore, a dual heat source (solar and biomass) can be used for Stirling engines to increase their conformity with nature [1].

Another important issue to threaten humanity is the dust explosion phenomenon. This phenomenon occurs in wheat silos and also in industries associated with micro-scale particles. A dust explosion is likely to occur when a finely divided combustible solid (in practice, the mean diameter of the particles should not exceed 1 mm) happens to be dispersed as a cloud in the air (with a typical mass loading between 10 and 1000 grams of dust per cubic meter or cloud), and when an appropriate ignition source (hot body, flame, electrical or mechanical spark, etc.) is activated inside this mixture. The heat evolved from the ignition source initiates the combustion of the particles located

---

[1] *Present address: Department of Mechanical Engineering, Faculty of Engineering, Arak University, Arak, 38156-88349, Iran.*

[*] *Corresponding author. Tel.: +98 21 77240540; Fax: +98 21 77240488*
*E-mail addresses: Bidabadi@iust.ac.ir (M. Bidabadi), Mostafavi@iust.ac.ir and a-mostafavi@araku.ac.ir (S.A. Mostafavi), Beidaghy_Hossein@MechEng.iust.ac.ir (H. Beidaghy Dizaji) and Farzadfaraji@MechEng.iust.ac.ir (F. Faraji Dizaji)*

in the vicinity of the ignition point. These particles, themselves, act as an ignition source for the adjacent slabs of the mixture, so that a 'combustion zone' is allowed to propagate without additional input of energy throughout the cloud. This 'combustion zone' has generally a finite thickness and is called the 'flame' [2].

A combustible dust explosion hazard may exist in a variety of industries, including: food (e.g. candy, starch, flour, feed), plastics, wood, rubber, furniture, textiles, pesticides, pharmaceuticals, dyes, coal, metals (e.g. aluminum, chromium, iron, magnesium, and zinc), and fossil fuel power generation. The vast majority of natural and synthetic organic materials, as well as some metals, can form combustible dust. Any industrial process that reduces a combustible material and some normally noncombustible materials to a finely divided state present a potential for a serious fire or explosion [3].

The most common dust explosion occurs in underground coal mines. In a coal mine tunnel, coal dust explosion is usually caused by gas explosion. Moving at the speed of sound, pressure wave resulting from a gas explosion lifts the deposited coal dust in the air. Then, the gas flame reaches the coal dust, causing a dust explosion, which is more severe than the original [4]. In order to have a better understanding of the process of generating heat and power from micro-biomass particles in Stirling engines, and also to predict a dust explosion phenomenon and it's severity, it is essential to study the combustion process of micro organic dust.

Lycopodium has been known as a reference particle in organic dust combustion studies since it is monosize, which is a basic assumption in analytical models [5,6]. Researchers have done many studies about lycopodium dust combustion, both experimentally [7-9] and analytically [10-12]. Han et al. [7] used the Thermal Gravity Analysis test (TGA) to achieve the combustive properties of lycopodium particles, and also calculate the burning velocity, flame temperature and flame length. Proust [8] reported the burning velocity and flame temperature for three different particles; lycopodium, starch and sulphur. Two methods for determining laminar burning velocities have been used: the classical 'tube method' and a 'direct method', based on the simultaneous determination of the flame speed and the mixture velocity ahead of the flame front, using a tomographic technique. Seshadri et al. [10] studied, analytically, the structure of premixed flames propagating in combustible systems, containing uniformly distributed volatile fuel particles, in an oxidizing gas mixture. Bidabadi et al. [11] presented an analytical model for lycopodium dust combustion considering temperature difference between the gas and particles.

In this research, an analytical model is used to calculate the flame characteristics of lycopodium particles, including the effect of char yield, which has not been previously considered. In previous studies [5,6,10,11,13], it is assumed that the only product of the pyrolysis procedure of the lycopodium particle is methane gas. However, it is not a precise assumption, because when an organic particle is exposed to heat sources, it is cracked into gas, liquid and solid phases that are named, respectively, gas, tar and char [14-17]; tar, eventually, converting into gas and char. In this article, our organic sample is the lycopoduim particle, 90% of which converts to methane gas when it is pyrolyzed. Other remained components of the lycopodium particle are converted to char, but tar production is neglected, since tar itself consequently cracks into methane and char.

To analyze the combustion of organic dust, the flame structure is divided into three zones. The first zone is the preheat zone, where the rate of chemical reaction is small. The second zone is an asymptotically thin reaction zone, where convection and the rate of vaporization of the particles are negligible in comparison with the reaction rate, and, finally, there is a post-flame zone. In next section, the conservation equations and required state equations needed to formulate the phenomenon are completely described. At the end, we compare our results with experimental results, and it is shown that our results are in reasonable agreement with the experimental results of Proust [8] and Wingerden et al. [9].

## 2. Governing equations

A one-dimensional steady model is used to simulate the combustion of organic dust, the flame of which is propagated in a uniformly distributed mixture of fuel particles. The initial density of the particles is $n_u$ and the initial radius of the particles is $r_u$. Biomass pyrolysis involves numerous extremely complex reactions with many intermediate and final products. According to this, many models of biomass degradation have been presented by different scientists [18]. In this study, a new model is presented to analyze the lycopodium organic dust flame. Also, a one step global pyrolysis model is used in which it is presumed that organic fuel decomposes into volatiles (gas) and carbon (char).

Since a large percent of produced gas is methane, the gas properties are considered the same as methane. Also, it is assumed that fuel mixture properties are calculated based on the mass fraction of methane and carbon in the mixture. It is also presumed that by burning the fuel mixture in an air oxidizer bed, $CO_2$ and $H_2O$ will be the products of combustion. Figure 1 shows a schematic figure of the flame structure divided into three zones: preheat zone, reaction zone and post flame zone.

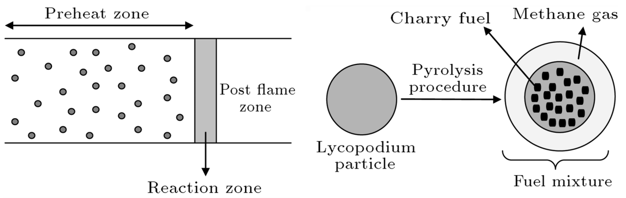

**Figure 1.** The flame structure of dust particles.

Reaction occurs in a thin zone, $O(\varepsilon)$, whereas preheat and post flame zones have considerable length. This assumption is based on asymptotic flame analysis or high Zeldovich number, and $\varepsilon$ is defined as a reciprocal of the Zeldovich number.

Mass conservation, organic particle mass conservation (solid particles) and fuel mixture conservation equations, along with energy conservation equations, are used to formulate the physical phenomena of solid particle combustion. Furthermore, the equation of state of the fuel mixture is used to restrict the equations in an atmospheric combustion condition to create a unique solution to our problem [10].

Since solid organic particles crack into gas and char when they are exposed to heat, summation of the fractions is equal to unity $(v_{s-g} + v_{s-c}) = 1$, which means that the fuel mixture is only a combination of gaseous and chary fuel. $v_{s-g}$ and $v_{s-c}$ are the gaseous fuel and chary fuel fractions of the solid particle.

## 3. Nondimensionalization of governing equations

These parameters are used to nondimensionalize governing equations:

$$\theta = \frac{(T - T_u)}{(T_f - T_u)}, \quad y_F = \frac{Y_F}{Y_{Fc}}, \quad y_s = \frac{Y_s}{Y_{Fc}},$$

$$m = \frac{\rho V}{\rho_u V_u} = 1, \quad Z = \frac{\rho_u V_u C}{\lambda_u} x. \tag{1}$$

In the above equation, $T_f$ is flame temperature and $Y_{Fc}$ is defined as:

$$Y_{Fc} Q = C(T_f - T_u). \tag{2}$$

Finally, these dimensionless quantities are defined:

$$\omega_g = \frac{\lambda_u w_g}{(\rho_u V_u)^2 C Y_{Fc}}, \quad \omega_c = \frac{\lambda_u w_c}{(\rho_u V_u)^2 C Y_{Fc}},$$

$$y_s = \frac{4\pi n_s \rho_s r^3}{3\rho Y_{Fc}}, \quad Q = \frac{Q_{pyr}}{Q},$$

$$\gamma = \frac{4.836 A {n_u}^{1/3} \lambda_u (T_f - T_u)^n}{V_u^2 {\rho_u}^{4/3} C {Y_{Fc}}^{1/3} {\rho_s}^{2/3}}. \tag{3}$$

In the above equations, $V_u$ is burning velocity. The Lewis number for the fuel mixture, and the ratio of the diffusion of heat to mass diffusion, is defined as below:

$$Le = \frac{\lambda_u}{\rho_u D_u C}. \tag{4}$$

It is supposed that $q$ has a negligible quantity (close to zero), which means that released heat from the reaction is greater than the heat absorbed by the particles for devolatilization. In this case, we replace $\theta$ with $\theta^\circ$. Thus, dimensionless equations yield:

$$\frac{d\theta^\circ}{dZ} = \frac{d^2\theta^\circ}{dZ^2} + (\omega_g + \omega_c)\frac{\rho_u}{\rho},$$

$$\frac{dy_F}{dZ} = \frac{1}{Le}\frac{d^2 y_g}{dZ^2} + \gamma {y_s}^{\frac{2}{3}} \theta^{\circ n} - (\omega_g + \omega_c)\frac{\rho u}{\rho}, \tag{5}$$

$$\frac{dy_s}{dZ} = -\gamma {y_s}^{\frac{2}{3}} \theta^{\circ n}.$$

The above equations are solved in each zone according to their boundary conditions and appropriate assumptions in order to obtain a reliable model for organic dust combustion and to predict flame characteristics.

## 4. Solution of governing equation in each zone

### *4.1. Preheat zones* $(-\infty < Z < 0)$

In the asymptotic solution, $(\varepsilon \to 0)$, it is possible to neglect the reaction term, because, in the preheat zone, particles pyrolyze to yield a mixture of gaseous and chary fuel and there is no reaction. The energy equation and boundary conditions are:

$$\frac{d\theta^\circ}{dZ} = \frac{d^2\theta^\circ}{dZ^2}, \quad Z = 0 \to \theta^\circ = 1, \quad Z = -\infty \to \theta^\circ = 0. \tag{6}$$

By solving the above equation, the nondimensional temperature distribution is:

$$\theta^\circ = \exp(Z), \quad Z \leq 0. \tag{7}$$

The mass conservation equation of organic particles converts to:

$$\frac{dy_s}{dZ} = -\gamma y_s^{\frac{2}{3}} [\exp(Z)]^n Z = -\infty \to y_s = \frac{Y_{Fu}}{Y_{Fc}} = \alpha. \tag{8}$$

$Y_{Fu}$, in the above equation, is the amount of fuel mixture that is available in the initial particles.
Thus:

$$y_s = [\alpha^{\frac{1}{3}} - \alpha e^{nZ}]^3, \tag{9}$$

$a$, in the above equation, is defined in the terms below:

$$a = \frac{\gamma}{3n}. \tag{10}$$

Thus, the conservation equation of the fuel mixture is changed to:

$$\frac{dy_F}{dZ} = \frac{1}{Le}\frac{d^2y_F}{dZ^2} + \gamma[\alpha^{\frac{1}{3}} - ae^{nZ}]^2e^{nZ}. \tag{11}$$

Boundary conditions are:

$$Z = -\infty \rightarrow y_F = 0, \quad Z = 0^- \rightarrow y_F = 0. \tag{12}$$

Finally, by solving the fuel mixture equation, the following equation is obtained:

$$\begin{aligned} y_F =& C_1e^{\mathrm{Le}.Z} - \frac{\mathrm{Le}.\gamma\alpha^{\frac{2}{3}}}{n^2 - n\mathrm{Le}}e^{nZ} + \frac{2\mathrm{Le}.\gamma a\alpha^{\frac{1}{3}}}{4n^2 - 2n\mathrm{Le}}e^{2nZ} \\ &- \frac{\mathrm{Le}.\gamma a^2}{9n^2 - 3n\mathrm{Le}}e^{3nZ}. \end{aligned}$$

$$C_1 = \frac{\mathrm{Le}.\gamma\alpha^{\frac{2}{3}}}{n^2 - n\mathrm{Le}} - \frac{2\mathrm{Le}.\gamma a\alpha^{\frac{1}{3}}}{4n^2 - 2n\mathrm{Le}} + \frac{\mathrm{Le}.\gamma a^2}{9n^2 - 3n\mathrm{Le}}, \tag{13}$$

and:

$$-\left[\frac{dy_F}{d_Z}\right]_{0^-} = \mathrm{Le}[3a\alpha^{\frac{2}{3}} + a^3 - 3a^2\alpha^{\frac{1}{3}}]. \tag{14}$$

### *4.2. Post flame zone* ($0 < Z < +\infty$)

Before analyzing the reaction zone, the post-flame zone is primarily investigated.

$$\theta = 1, \quad y_s = \text{constant}, \quad y_F = 0. \tag{15}$$

In the post-flame zone, the available mass fraction of solid particles is approximately equal to the quantity of $y_s$ at the end of the vaporization zone (i.e. Z = $0^-$)

### *4.3. Reaction zone (Z = o)*

In this zone, the rate of reaction is considerable, and convection and devolatilization terms are negligible in comparison with diffusion and reaction terms. It means:

$$\frac{d\theta^\circ}{dZ} \approx 0, \qquad \frac{dy_F}{dZ} \approx 0, \qquad \gamma {y_s}^{\frac{2}{3}}\theta^{\circ n} \approx 0. \tag{16}$$

Governing equations in this zone convert into the following equations:

$$\frac{dy_s}{dZ} = 0 \rightarrow y_s = \mathrm{cte},$$

$$\frac{d^2\theta^\circ}{dZ^2} = -(\omega_g + \omega_c)\frac{\rho_u}{\rho},$$

$$\frac{d^2y_F}{dZ^2} = \mathrm{Le}.(\omega_g + \omega_c)\frac{\rho_u}{\rho}. \tag{17}$$

In the above equations, gaseous and chary fuel reaction rates are defined as:

$$\omega_g = \frac{\lambda_u w_g}{(\rho_u V_u)^2 CY_{Fc}}, \qquad \omega_c = \frac{\lambda_u w_c}{(\rho_u V_u)^2 CY_{Fc}},$$

$$w_g = v_g W_g k_g C_g, \qquad w_c = v_c W_c k_c C_c,$$

$$k_g = B_g \exp\left(-\frac{E_g}{RT}\right), \qquad k_c = B_c \exp\left(-\frac{E_c}{RT}\right). \tag{18}$$

Subscripts $c$ and $g$ denote char and gas and $C$, $W$ and $k$ are the molar concentration, molecular weight and the constant rate of the overall reaction, respectively. $v$ is the stoichiometric coefficient of the fuel components, which represents the amount of produced gas and char in the devolatilization process:

$$v_g = v_{s-g} \text{ and } v_c = v_{s-c}. \tag{19}$$

In order to analyze the reaction zone expansion parameter, $\varepsilon = \frac{1}{Ze}$ is defined to expand the reaction zone. By using $\varepsilon$, all our previous parameters are expanded and rewritten as:

$$\eta = \frac{Z}{\varepsilon}, \qquad y^* = \frac{y_F - y_{F_F}}{\varepsilon}, \qquad t = \frac{1 - \theta^\circ}{\varepsilon}. \tag{20}$$

$y_{F_F}$ is the mass fraction of the fuel mixture prior to the reaction zone. Using the above expanded parameters, conservation Eq. (17) are rewritten as follows:

$$\frac{d^2t}{d\eta^2} = \varepsilon(\omega_g + \omega_c)\frac{\rho_u}{\rho},$$

$$\frac{d^2y^*}{d\eta^2} = \varepsilon\mathrm{Le}.(\omega_g + \omega_c)\frac{\rho_u}{\rho}. \tag{21}$$

Solving the above equations, burning velocity is achieved, which is the primary purpose of this article.

$$\begin{aligned} V_u^2 =& 2\varepsilon^2\mathrm{Le}.D_{uF}\left[\left\{v_g B_g.\exp\left(-\frac{E_g}{RT_f}\right)\right.\right. \\ &\left.\left. + v_c B_c.\exp\left(-\frac{E_c}{RT_f}\right)\right\}.(\mathrm{Le} + b)\right]. \end{aligned} \tag{22}$$

According to Eq. (22), burning velocity is a function of $T_f$, which is an indeterminate parameter. We need another expression in order to simultaneously solve these two expressions and calculate indeterrminate parameters. In the resumption, the process of finding this expression is explained.

In Eq. (17), by combining each side of the energy, gaseous fuel and chary fuel conservation equations together, the following equation is produced:

$$\frac{d^2\theta^\circ}{dZ^2} + \frac{1}{\mathrm{Le}}\frac{d^2y_F}{dZ^2} = 0. \tag{23}$$

By integrating Eq. (23) from $Z = 0^-$ to $Z = 0^+$, it is possible to achieve the following matching condition:

$$\left[\frac{d\theta^\circ}{dZ}\right]_{0^-}+\frac{1}{\mathrm{Le}}\left[\frac{dy_F}{dZ}\right]_{0^-}=0. \tag{24}$$

Finally, by substituting Eqs. (7) and (14) into Eq. (24), the following expression, which connects burning velocity and flame temperature, is achieved:

$$3a\alpha^{\frac{2}{3}}+a^3-3a^2\alpha^{\frac{1}{3}}-1=0. \tag{25}$$

## 5. Results and discussion

In order to predict flame characteristics, like burning velocity and mass fractions of a generated fuel mixture, the explicit expression for the burning velocity in Eq. (22) should be solved, simultaneously, with Eq. (25). To evaluate the accuracy of the presented model, the obtained burning velocity is compared with the flame velocity, which is calculated by Proust [8] and Van Wingerden et al. [9]. Proust calculated the burning velocity of lycopodium as a function of mass particle concentration in both the direct and tube methods. To compare our results with experimental data, we require some initial data, like $r_p = 15.5$ $\mu$m and $v_{s-g} = 0.9$, which are related to the physical and chemical characteristics of lycopodium particles. As shown in Figure 2, it is understood that our result is in reasonable agreement with experimental data.

In gas flame analysis, two types of resistance exist against flame propagation; heat transfer resistance and chemical reaction resistance. In dry dust flame, pyrolysis (devolatization) resistance is also added to these resistances. In fact, the interactions between these resistances in each flame control the flame characteristics like burning velocity and flame temperature. It is clear that mass transfer resistance exists in all types of the above flames.

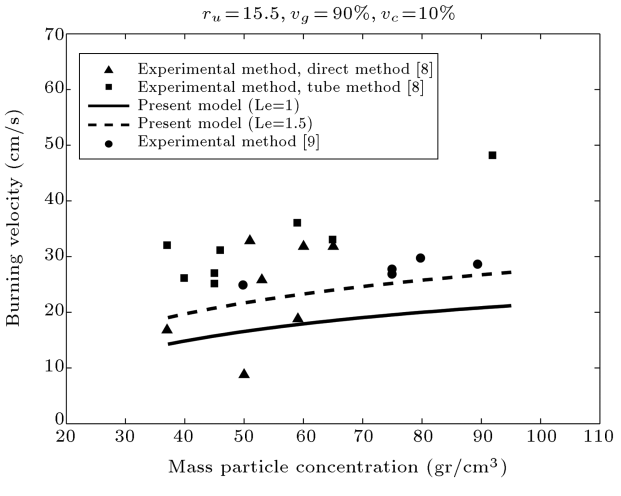

**Figure 2.** The variation of burning velocity as a function of mass particle concentration for both the present model and experimental data [8,9].

As shown in Figure 3, it is clear that by increasing char content, the adiabatic flame temperature of the fuel mixture, $CH_4$ + C, which is obtained from thermodynamics, increases. This happens because the energy density of chary fuel is higher than methane fuel. It is notable that in measuring adiabatic temperature, the rate of reaction is neglected. The only factor that affects adiabatic temperature is the combustion heat, which is related to the enthalpy of formation. Also, it is understood that by increasing the equivalence ratio, adiabatic temperature decreases due to an excessive amount of fuel, which remains unburned because of an insufficient oxidizer.

On the other hand, as shown in Figure 4, an increase in char content causes a decrease in burning velocity. In fact, a carbon particle has fewer tendencies to react with oxygen in comparison with methane,

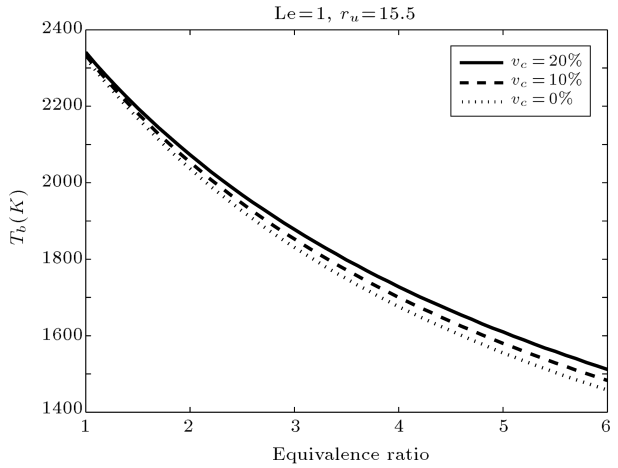

**Figure 3.** The variation of adiabatic flame temperature as a function of equivalence ratio ($\varphi_u$) for different char contents.

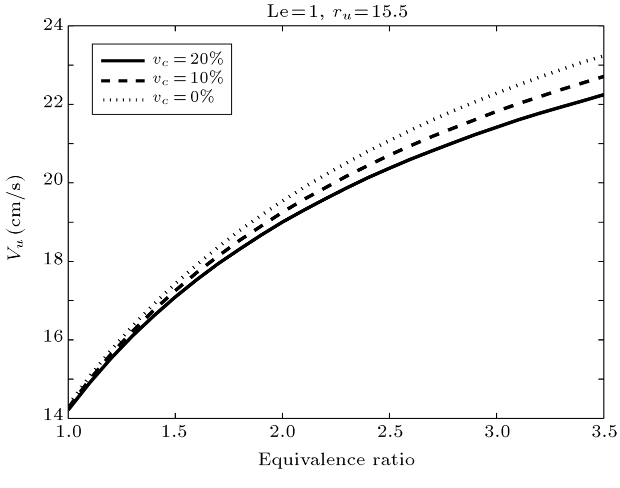

**Figure 4.** The variation of burning velocity as a function of equivalence ratio for different char contents.

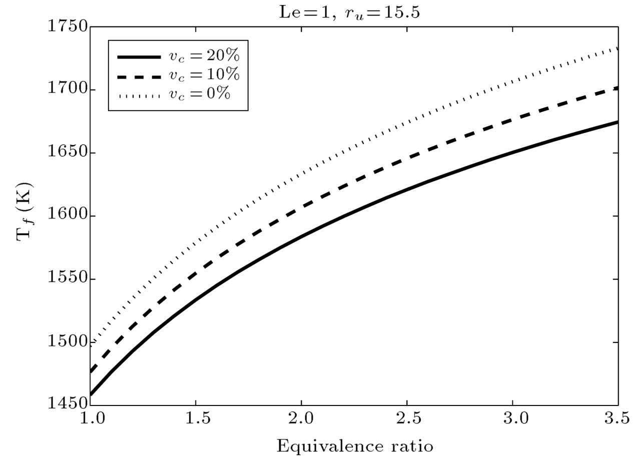

**Figure 5.** The variation of flame temperature as a function of equivalence ratio for different char contents.

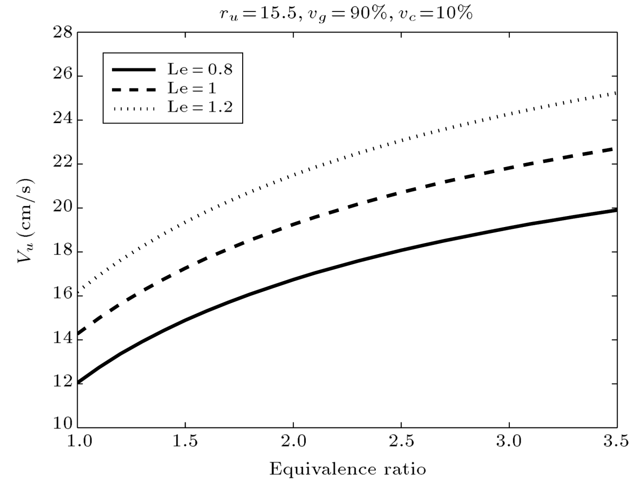

**Figure 6.** The variation of burning velocity as a function of equivalence ratio for different Lewis number.

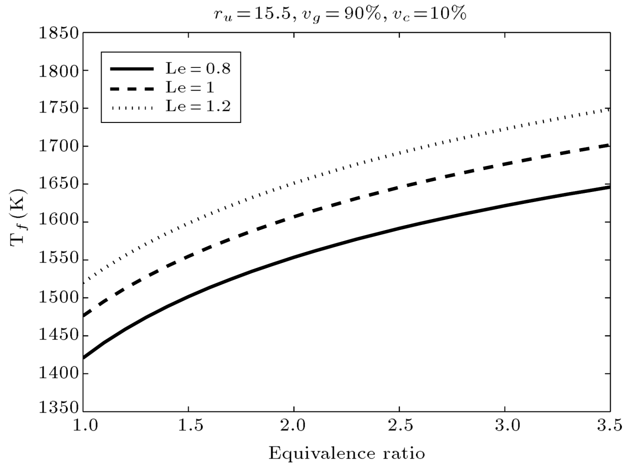

**Figure 7.** The variation of flame temperature as a function of equivalence ratio for different Lewis number.

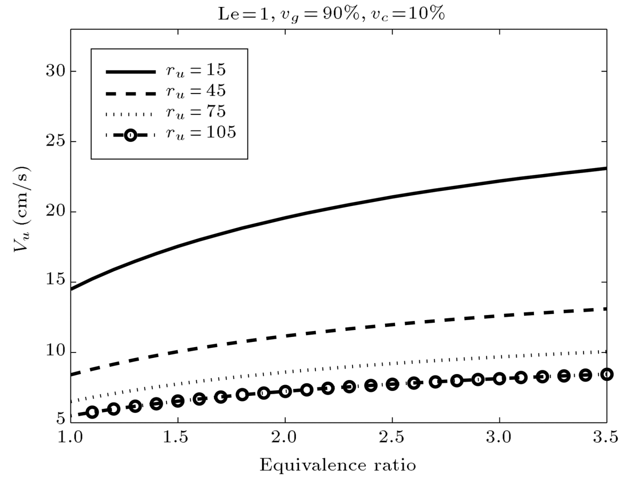

**Figure 8.** The variation of burning velocity as a function of equivalence ratio for different particle radius.

due to the solid structure of carbon. Furthermore, according to Figure 5, by increasing char content, flame temperature decreases.

The Lewis number variation (ratio of thermal diffusivity to mass diffusivity) has a strong effect on the burning velocity. An increase in Lewis number is associated with a noticeable rise in thermal diffusivity. This improves the pyrolysis condition in the preheat zone, due to an increase in the amount of induced heat from the reaction zone into the preheat zone. As a result, burning velocity is increased, which is shown in Figure 6.

The Lewis number has also a dual effect on generated gaseous fuel. At first, an increase in Lewis number accelerates the vaporization process of solid fuel particles, due to an intense increase in the thermal diffusivity effect. On the other hand, an increase in Lewis number is associated with a sharp reduction in mass diffusivity, which implies that the combustion condition has deteriorated. However, it is clearly understood that thermal diffusivity has a dominant effect, which increases in Lewis number, causing an increase in burning velocity. Also, by increasing Lewis number, flame temperature increases, as shown in Figure 7.

Finally, the effect of particle radius on flame properties has been investigated. By decreasing the particle radius effective surface, the surface exposed to heat increases and, eventually, improves the pyrolysis process, which increases the amount of generated fuel mixture. As shown in Figure 8, burning velocity is increased by reducing particle size. Again, a similar trend is observed for flame temperature, illustrated in Figure 9.

## 6. Conclusion

In this study, an analytical model for the combustion of a lycopodium dust cloud is presented to determine the effect of char content. Furthermore, the effect

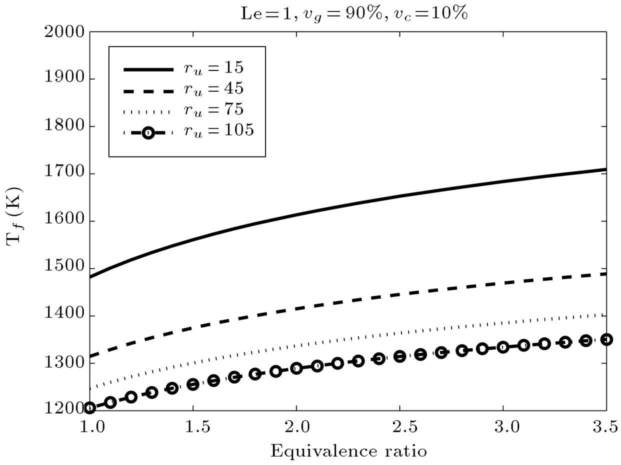

**Figure 9.** The variation of burning velocity as a function of equivalence ratio for different particle radius.

of different parameters, like particle size and Lewis number, is also investigated. From obtained results, it is understood that an increase in char content causes a reduction in burning velocity, but a reverse trend is observed in the adiabatic temperature of the flame. These contrary trends can be explained by distinguishing between available energy in the chary fuel and its tendency to react. Chary fuel has more energy compared to methane gas, but it has a lower tendency to react. So, a higher adiabatic temperature is achieved, while burning velocity decreases. Additionally, flame temperature, which is coupled with burning velocity, also decreases. It is notable that burning velocity and flame temperature have a similar trend when a parameter is varied. Also, the effect of Lewis number and particle radius are also investigated. An increase in Lewis number improves the pyrolysis procedure of organic dust and, consequently, burning velocity increases. Besides, a reduction in particle radius increases the amount of generated fuel mixture, which increases burning velocity.

## Nomenclature

| | |
|---|---|
| $A$ | Parameter characterizing rate of devolatilization of fuel particles |
| $a$ | Defined in Eq. (10) |
| $B_g$ | Frequency factor characterizing rate of gas phase oxidation |
| $B_g$ | Frequency factor characterizing rate of solid phase oxidation |
| $b = \frac{y_{FF}}{\varepsilon}$ | Scaled mass fraction of fuel at the boundary between the reaction zone |
| $C$ | Heat capacity of mixture |
| $C_g$ | Molar concentration of gas |
| $C_c$ | Molar concentration of char |
| $C_F$ | Molar concentration of fuel mixture |
| $C_p$ | Heat capacity of the gas |
| $C_s$ | Heat capacity of a fuel particle |
| $D$ | Diffusion coefficient |
| $E_g$ | Activation energy characterizing the gas reaction, Eq. (18) |
| $E_c$ | Activation energy characterizing the char reaction, Eq. (18) |
| $k_g$ | Rate constant of the gas reaction |
| $k_c$ | Rate constant of the char reaction |
| Le | Lewis number, Eq. (4) |
| $m$ | Defined in Eq. (1) |
| $n$ | Temperature exponent characterizing rate of devolatilization of fuel particles |
| $n_s$ | Local number density of particles (number of particles per unit volume) |
| $n_u$ | Local number density of particles (number of particles per unit volume) |
| $Q$ | Heat release per unit mass of gas and char fuel consumed |
| $Q_{pyr}$ | Heat associated with devolatilizing unit mass of fuel |
| $q$ | Defined in Eq. (3) |
| $R$ | Gas constant |
| $r$ | Radius of fuel particle |
| $T$ | Temperature |
| $t$ | Defined in Eq. (20) |
| $V$ | Velocity |
| $V_u$ | Burning velocity (Eq. 22) |
| $v_{s-c}$ | Char yield |
| $v_{s-g}$ | Gas yield ($v_{s-g} + v_{s-c} = 1$ |
| $W_c$ | Molecular weight of char |
| $W_g$ | Molecular weight of gaseous fuel |
| $w_c$ | Reaction rate characterizing consumption of char, Eq. (18) |
| $w_g$ | Reaction rate characterizing consumption of gaseous fuel, Eq. (18) |
| $w_{pyr}$ | Rate of devolatilization of fuel particles |
| $Y$ | Mass fraction |
| $Y_{Fc}$ | Defined in Eq. (2) |
| $Y_{Fu}$ | Gas and char fuel available in the particles in the ambient reactant stream |
| $y_F$ | Defined in Eq. (1) |
| $y_s$ | Defined in Eq. (1) |
| $y^*$ | Defined in Eq. (20) |
| Ze | Zeldovich number |

| | |
|---|---|
| $Z$ | Scaled independent variable, Eq. (1) |

*Greek Symbols*

| | |
|---|---|
| $\forall$ | Volume |
| $\alpha$ | $Y_{Fu}/Y_{Fc}$ |
| $\gamma$ | Defined in Eq. (3) |
| $\varepsilon$ | 1/Ze, expansion parameter |
| $\eta$ | Independent variable defined in Eq. (20) |
| $\theta$ | Defined in Eq. (1) |
| $\theta^{\circ}$ | Value of $\theta$ calculated neglecting the heat of devolatilization of particles |
| $\Lambda_g$ | Defined in Eq. (A.10) |
| $\Lambda_c$ | Defined in Eq. (A.10) |
| $\lambda$ | Thermal conductivity reactant mixture |
| $\rho$ | Density of reactant mixture |
| $\rho_s$ | Density of fuel particle |
| $v$ | Stoichiometric coefficient |
| $\varphi_u$ | Equivalence ratio, based on fuel available in the particles in the ambient reactant stream |
| $\omega_c$ | Defined in Eq. (3) |
| $\omega_g$ | Defined in Eq. (3) |

*Subsecripts*

| | |
|---|---|
| $b$ | Adiabatic conditions after completion of chemical reactions |
| $c$ | Char |
| $f$ | Conditions at the reaction zone |
| $F$ | Fuel mixture (methane+char) |
| $g$ | Gaseous fuel (methane) |
| $o_2$ | Oxygen |
| $s$ | Solid fuel particles |
| $u$ | Conditions in the ambient reactant stream |

## References

1. Zeiler, M., Podesser, E., Dermouz, H., Enzinger, P., Gunczy, S., Lauer, M., Padinger, R. and Wenzel, A. "Sustainable energy supply of an austrian winery based on solar and biomass driven microCHCP", *Proceedings of the 16th European Biomass Conference and Exhibition From Research to Industry and Markets Valencia*, Spain, (2008).
2. Proust, C. "Dust explosions in pipes: A review", *Journal of Loss Prevention in the Process Industries*, **9**(4), pp. 267-277 (1996).
3. National Fire Protection Association (NFPA) "Industrial fire hazards handbook", 3rd Ed., NFPA Inc. (1990).
4. Yan-song Zhang, Li-li Han and Lei Wang "Mechanism research of gas and coal dust explosion", *Journal of Coal Science & Engineering*, **15**(2), pp. 171-174 (2009).
5. Bidabadi, M. and Rahbari, A. "Novel analytical model for predicting the combustion characteristics of premixed flame propagation in lycopodium dust particles", *Journal of Mechanical Science and Technology*, **23**, pp. 2417-2423 (2009).
6. Bidabadi, M., Haghiri, A. and Rahbari, A. "The effect of Lewis and Damköhler numbers on the flame propagation through micro-organic dust particles", *International Journal of Thermal Sciences*, **49**, pp. 534-542 (2010).
7. Han, O.S., Yashima, M., Matsuda, T., Matsui, H., Miyake, A. and Ogawa, T. "Behavior of flames propagating through lycopodium dust clouds in a vertical dust", *Journal of Loss Prevention in the Process Industries*, **13**, pp. 449-457 (2000).
8. Proust, C. "Flame propagation and combustion in some dust-air mixtures", *Journal of Loss Prevention in the Process Industries*, **19**, pp. 89-100 (2006).
9. Van Wingerden, K., Stavseng, L. and Bergen, N. "Measurements of the laminar burning velocities in dust-air mixtures", http://www2.gexcon.com/download/VDI2.pdf.
10. Seshadri, K., Berlad, A.L. and Tangirala, V. "The structure of premixed particle-cloud flames", *Combustion and Flame*, **89**, pp. 333-342 (1992).
11. Bidabadi, M. and Rahbari, A. "Modeling combustion of lycopodium particles by considering the temperature difference between the gas and the particles", *Combustion, Explosion and Shock Waves*, **45**(3), pp. 278-285 (2009).
12. Bidabadi, M., Shakibi, A. and Rahbari, A. "The radiation and heat loss effects on the premixed flame propagation through lycopodium dust particles", *Journal of the Taiwan Institute of Chemical Engineers*, **42**, pp. 180-185 (2011).
13. Haghiri, A. and Bidabadi, M. "Modeling of laminar flame propagation through organic dust cloud with thermal radiation effect", *International Journal of Thermal Sciences*, **49**, pp. 1446-1456 (2010).
14. Di Blasi, C. "Analysis of convection and secondary reaction effects within porous solid fuels undergoing pyrolysis", *Combustion Science and Technology*, **90**, pp. 315-340 (1993).
15. Vijeu, R., Gerun, L., Tazerout, M., Castelain, C. and Bellettre, J. "Dimensional modelling of wood pyrolysis using a nodal approach", *Fuel*, **87**, pp. 3292-3303 (2008).
16. Bryden, K.M., Ragland, K.W. and Rutland, C.J. "Modeling thermally thick pyrolysis of wood", *Biomass and Bioenergy*, **22**, pp. 41-53 (2002).
17. Mousques, P. "Modelisation du couplage des reactions chimiques-transferts de chaleur/matiere en vue du dimensionnement des reacteurs de pyrolyse", PhD Thesis, Universite de Perpignan (2001).

18. Prakash, N. and Karunanithi, T. "Advances in modeling and simulation of biomass pyrolysis", *Asian Journal of Scientific Research*, pp. 1-27 (2009).

## Appendix

By substituting $w_g$ and $w_c$ in Eq. (3), the following equations are achieved:

$$\omega_g = \frac{\lambda_u v_g W_g C_g B_g}{(\rho_u V_u)^2 C Y_{Fc}} \exp\left(\frac{-E_g}{RT}\right),$$

$$\omega_c = \frac{\lambda_u v_c W_c C_c B_c}{(\rho_u V_u)^2 C Y_{Fc}} \exp\left(\frac{-E_c}{RT}\right). \tag{A.1}$$

In order to solve our equations, $(\frac{E}{RT})$ should be converted into $((\frac{E}{RT_f}) + t)$. This process is explained in the following equations:

$$\frac{E}{RT} = \frac{E}{R(T - T_f + T_f)} \xrightarrow{\alpha = T_f - T} \frac{E}{RT} = \frac{E}{R(T_f - \alpha)}$$

$$= \frac{E(T_f + \alpha)}{R(T_f^2 + \alpha^2)} \xrightarrow{\alpha^2 \approx 0} \frac{E}{RT} = \frac{E}{RT_f} + \frac{E\alpha}{RT_f^2}. \tag{A.2}$$

By using $\text{Ze} = (\frac{1}{\varepsilon})$, the following equation is obtained:

$$\text{Ze} = \frac{E(T_f - T_u)}{RT_f^2} = \frac{1}{\varepsilon} \to \frac{E}{RT_f^2} = \frac{1}{\varepsilon(T_f - T_u)}. \tag{A.3}$$

Then, Eqs. (A.2) and (A.3) are combined:

$$\frac{E\alpha}{RT_f^2} = \frac{\alpha}{\varepsilon(T_f - T_u)} = \frac{T_f - T}{\varepsilon(T_f - T_u)},$$

$$\frac{T_f - T}{T_f - T_u} = 1 - \frac{T - T_u}{T_f - T_u} \xrightarrow{Eq.(1)} \frac{T_f - T}{T_f - T_u} = 1 - \theta^\circ,$$

$$\frac{E\alpha}{RT_f^2} = \frac{1 - \theta^\circ}{\varepsilon} \xrightarrow{Eq.(20)} \frac{E\alpha}{RT_f^2} = t. \tag{A.4}$$

Finally, by substituting Eq. (A.4) in Eq. (A.2), the following relation is achieved:

$$\frac{E}{RT} = \frac{E}{RT_f} + t \to \begin{cases} -\frac{E_g}{RT} = -\frac{E_g}{RT_f} - t \\ -\frac{E_c}{RT} = -\frac{E_c}{RT_f} - t \end{cases}. \tag{A.5}$$

By substituting Eq. (A.5) into Eq. (A.1), the last abstract mathematical problem is finished and we return to the primary problem and its solution:

$$\omega_g = \frac{\lambda_u v_g W_g C_g B_g}{(\rho_u V_u)^2 C Y_{Fc}} \exp\left(-\frac{E_g}{RT_f} - t\right),$$

$$\omega_c = \frac{\lambda_u v_c W_c C_c B_c}{(\rho_u V_u)^2 C Y_{Fc}} \exp\left(-\frac{E_c}{RT_f} - t\right). \tag{A.6}$$

By substituting Eq. (A.6) in the energy conservation equation (Eq. (21)), it is rewritten in the following terms:

$$\frac{d^2 t}{d\eta^2} = \frac{\rho_u}{\rho} \varepsilon \left\{ \frac{\lambda_u v_g W_g C_g B_g}{(\rho_u V_u)^2 C Y_{Fc}} \exp\left(-\frac{E_g}{RT_f} - t\right) \right.$$

$$\left. + \frac{\lambda_u v_c W_c C_c B_g}{(\rho_u V_u)^2 C Y_{Fc}} \exp\left(-\frac{E_c}{RT_f} - t\right) \right\}$$

$$\xrightarrow{(\text{Le} = \frac{\lambda_u}{\rho_u D_u C})} \frac{d^2 t}{d\eta^2}$$

$$= \frac{\varepsilon.\text{Le}.D_{uF}}{\rho V_u^2 Y_{Fc}} \left\{ (v_g W_g C_g B_g).\exp\left(-\frac{E_g}{RT_f} - t\right) \right.$$

$$\left. + (v_c W_c C_c B_c).\exp\left(-\frac{E_c}{RT_f} - t\right) \right\}. \tag{A.7}$$

Now, using the following equations from Eqs. (1) and (20), it is possible to find another expression for $Y_F c$, which is used in Eq. (A.7):

$$y^* = \frac{y_g - y_{F_F}}{\varepsilon} \to y_F = \varepsilon y^* + y_{F_F} \xrightarrow{b = (y_{F_F}/\varepsilon)} y_F$$

$$= \varepsilon(y^* + b),$$

$$Y_F = \frac{m_F}{m_F + m_{\text{air}}} = \frac{m_g + m_c}{m_g + m_c + m_{\text{air}}}$$

$$= \frac{m_F}{m} \to Y_F = \frac{\rho_F \forall_F}{\rho \forall} = \frac{\rho_F}{\rho} = \frac{W_F C_F}{\rho},$$

$$Y_{Fc} = \frac{Y_F}{y_F} = \frac{Y_F}{\varepsilon(y^* + b)} \to Y_{Fc} = \frac{W_F C_F}{\rho \varepsilon (y^* + b)}. \tag{A.8}$$

It is possible to calculate $b$, which is used in the above equations, using the following equations:

$$b = \frac{y_F|_{Z=-\varepsilon}}{\varepsilon} = \text{Ze}.\text{Le}\left[ \frac{\gamma \alpha^{\frac{2}{3}}}{n^2 - n\text{Le}} (e^{-\frac{\text{Le}}{\text{Ze}}} - e^{\frac{n}{\text{Ze}}}) \right.$$

$$- \frac{2\gamma a \alpha^{\frac{1}{3}}}{4n^2 - 2n\text{Le}} (e^{-\frac{\text{Le}}{\text{Ze}}} - e^{-\frac{2n}{\text{Ze}}})$$

$$\left. + \frac{\gamma a^2}{9n^2 - 3n\text{Le}} (e^{-\frac{\text{Le}}{\text{Ze}}} - e^{\frac{3n}{\text{Ze}}}) \right]. \tag{A.9}$$

By substituting the above expressions in Eq. (A.7) and rewriting it, the following equation is obtained:

$$\frac{d^2 t}{d\eta^2} = [(\Lambda_g + \Lambda_c)(y^* + b)] \exp(-t),$$

$$\Lambda_g = \frac{\varepsilon^2.\text{Le}.D_{u_F}}{V_u^2} \left[ v_g B_g.\exp\left(-\frac{E_g}{RT_f}\right) \right],$$

$$\Lambda_c = \frac{\varepsilon^2.\text{Le}.D_{u_F}}{V_u^2} \left[ v_c B_c.\exp\left(-\frac{E_c}{RT_f}\right) \right]. \tag{A.10}$$

Combining Eq. (25) results in the following expression:

$$\begin{cases} \frac{d^2t}{d\eta^2} = \varepsilon(\omega_g + \omega_c)\frac{\rho_u}{\rho} \\ \frac{d^2y^*}{d\eta^2} = \varepsilon.\mathrm{Le}(\omega_g + \omega_c)\frac{\rho_u}{\rho} \end{cases} \xrightarrow{\text{yields}} \frac{d^2[t - \frac{1}{\mathrm{Le}}y^*]}{d\eta^2} = 0. \tag{A.11}$$

The boundary condition for the above equation is determined, via the boundary condition, when $\eta \to +\infty$, and the solution for the post-flame zone is determined as follows:

$$\frac{dt}{d\eta} = \frac{dt}{dZ} \times \frac{dZ}{d\eta} = \frac{d(\frac{1-\theta}{\varepsilon})}{dZ} \times \varepsilon = -\frac{d\theta}{dZ}$$

$$\to \frac{dt}{d\eta}|_{\eta\to+\infty} = -\frac{d\theta}{dZ}|_{Z\to 0^+} = -\frac{d(1)}{dZ}|_{Z\to 0^+} = 0, \tag{A.12}$$

$$\frac{dy^*}{d\eta} = \frac{dy^*}{dZ} \times \frac{dZ}{d\eta} = \frac{d(\frac{y_F - y_{F_F}}{\varepsilon})}{dZ} \times \varepsilon = -\frac{dy_F}{dZ}$$

$$\to \frac{dy^*}{d\eta}|_{\eta\to+\infty} = -\frac{dy_F}{dZ}|_{Z\to 0^+} = 0. \tag{A.13}$$

Integrating twice from Eq. (A.11) and utilizing the Expressions (A.12) and (A.13) lead to:

$$t = \frac{1}{Le}y^*. \tag{A.14}$$

By substituting the above relations in Eq. (A.10), the following equation is achieved:

$$\frac{d^2t}{d\eta^2} = [(\Lambda_g + \Lambda_c)(Le.t + b)]\exp(-t). \tag{A.15}$$

The boundary condition for variable t is determined from the $\theta$ boundary condition:

$$\frac{dt}{d\eta}|_{\eta\to-\infty} = -\frac{d\theta}{dZ}|_{Z\to 0^-} = -\frac{d(\exp(Z))}{dZ}|_{Z\to 0^-} = -1. \tag{A.16}$$

By, using the below substitution and rewriting Eq. (A.15) and using some mathematical operations, it is possible to obtain burning velocity:

$$P = \frac{dt}{d\eta} \to \frac{d^2t}{d\eta^2}$$

$$= P\frac{dp}{dt} \to \begin{cases} P|_{Z=0^-} = \frac{dt}{d\eta}|_{\eta\to-\infty} = -1 \\ P|_{Z=0^+} = \frac{dt}{d\eta}|_{\eta\to+\infty} = 0 \end{cases} \tag{A.17}$$

$$\theta = \left(\frac{T - T_u}{T_f - T_u}\right) \to 1 - \theta = \left(\frac{T_f - T}{T_f - T_u}\right) \xrightarrow{t=\frac{1-\theta}{\varepsilon}} t$$

$$= \left(\frac{1}{T_f - T_u}\right) \times \left(\frac{T_f - T_u}{\varepsilon}\right)$$

$$\to \begin{cases} t|_{Z=0^-} = \left(\frac{1}{T_f - T_u}\right) \times \left(\frac{T_f - (T_f^-)}{\varepsilon}\right) = +\infty \\ t|_{Z=0^+} = \left(\frac{1}{T_f - T_u}\right) \times \left(\frac{T_f - T_f}{\varepsilon}\right) = 0 \end{cases} \tag{A.18}$$

$$\xrightarrow{Eq.\,(A.15)} \mathrm{PdP} = \{[(\Lambda_g + \Lambda_c)(\mathrm{Le}.t + b)]\exp(-t)\}dt. \tag{A.19}$$

By integrating from Eq. (A.19), we have:

$$\left(\frac{P^2}{2}\right]_{-1}^{0} = [(\Lambda_g + \Lambda_c).\{[\mathrm{Le}.(-te^{-t} - e^{-t})].$$

$$- b.e^{-t}\}]]_{+\infty}^{0}. \tag{A.20}$$

Eventually, Eq. (A.20) is rewritten as:

$$\frac{1}{2} = (\Lambda_g + \Lambda_c).(\mathrm{Le} + b). \tag{A.21}$$

Now, after all complex mathematical operations, which are completely explained in the above relations, by substituting $\Lambda_g$ and $\Lambda_c$ in Eq. (A.10), the primary aim of this article, which is burning velocity, is written in the following expression:

$$V_u^2 = 2\varepsilon^2\mathrm{Le}.D_{u_F}\left[\left\{v_g B_g.\exp\left(-\frac{E_g}{RT_f}\right)\right.\right.$$

$$\left.\left. + v_c B_c.\exp\left(\frac{-E_c}{RT_f}\right)\right\}.(\mathrm{Le} + b)\right]. \tag{A.22}$$

## Biographies

**Mehdi Bidabadi** received his BS degree in Mechanical Engineering from Iran University of Science and Technology, where he is a faculty member, and MS and PhD degrees from Sharif University of Technology, Iran, and McGill University, Canada, respectively. His research interests include: dust flame propagation mechanisms, combustion, wind tunnels and gas dynamics, development of a new experimental apparatus to produce laminar flow and optimization of smoke wind tunnels. He has published several research papers in the field of dust combustion.

**Seyed Alireza Mostafavi** received a BS degree in Mechanical Engineering from Shahrood University of Technology, Iran, in 2004, an MS degree in Mechanical Engineering from Isfahan University of Technology, Iran, in 2008, and a PhD degree in Mechanical Engineering from Iran University of Science and Technology in 2013. He is a faculty member in the Mechanical Engineering Department at Arak University, Iran. His research interests include energy, combustion and the environment, especially numerical and experimental study of reactive fluid flow. He has published several research papers in these fields.

**Hossein Beidaghy Dizaji** received his BS degree in Mechanical Engineering from the Islamic Azad

University of Tabriz, Iran, in 2009, and his MS degree in Aerospace Engineering (Propulsion), in 2011, from Iran University of Science and Technology, where he is currently working in the Combustion Research Laboratory. His research interests include combustion, renewable energy (biomass and solar), internal combustion engines (included gas turbines), thermo fluid systems (power plants and cooling systems) and experimental fluid mechanics.

**Farzad Faraji Dizaji** received his BS degree in Mechanical Engineering from the University of Tabriz, in 2009, and his MS degree in Mechanical Engineering, in 2011, from Iran University of Science and Technology, where he is currently working in the Combustion Research Laboratory. His research interests include combustion and explosion, renewable energy (biomass and bio-fuel), internal combustion engines (included gas turbines) and experimental fluid mechanics.